07.3

Experimental implementation of reservoir computing with a semiconductor laser subject to optoelectronic feedback

© G.O. Danilenko, D.A. Pavlov, E.A. Viktorov, A.V. Kovalev

ITMO University, St. Petersburg, Russia
E-mail: avkovalev@itmo.ru

Received April 23, 2024
Revised May 8, 2024
Accepted May 13, 2024

We present the results of experimental research of a reservoir computing system based on a semiconductor laser with optoelectronic feedback. In the research, the memory capacity of the system and error in predicting the chaotic Mackey–Glass time series have been determined. The effect of the system pump current, feedback strength and number of nodes on its performance has been investigated.

Keywords: reservoir computing, semiconductor lasers, optoelectronic feedback.

DOI: 10.61011/TPL.2024.09.59147.19971

Reservoir computing (RC) is such an approach to machine learning, which is based on the dynamic system nonlinear response to the input signal. The RC systems are used for solving time-dependent problems and analyzing big data; their distinctive features are a simplified approach to the system training and energy efficiency in implementing it based on physical devices. There have already been experimentally demonstrated systems based on optoelectronic oscillators [1,2], optical-feedback (FB) semiconductor lasers [3], and photonic integrated circuits [4]. Among physical, and, in particular, optical implementations of RCs, systems with time delay (TDSs) [5] are especially common. The TDS basis is using a single nonlinear node and time-delayed FB. Along with this, time multiplexing is used to create N virtual nodes similar to those of recurrent neural networks, which are distributed in the FB circuit at fixed time intervals t_N [3,5].

In this work, the TDS system based on an optoelectronic-FB semiconductor laser, which was previously considered in theoretical works [6–8], has been studied experimentally; dependence of its memory capacity and error in predicting the chaotic time series on the system parameters have been determined.

Schematic diagram of the experimental setup is given in Fig. 1. This setup employs standard optical components with single-mode fiber leads with FC/APC connectors and is insensitive to changes in the optical field polarization state and phase. In implementing this approach, a single-frequency continuously emitting laser was used as a source of laser radiation. The modulation bandwidth of the laser pump current governs the frequency of entering data into the system and number of nodes, which are achievable in the system in question (see below). In this work, we used a distributed-feedback laser diode Nolatech DFB-1550-14BF (LD) with the wavelength of 1550 nm, threshold current of 9 mA, and output power of 5 mW at the current of 40 mA, whose temperature was stabilized by using temperature controller ELECDEMO KW_DFB (TC). LD was powered by a stabilized current source Keysight N6705C (CS). Laser radiation passed through the optical insulator (OI) and was recorded by photodetector Alphalas UPD-15-IR2-FC (PD); a part of the photodetector output signal was recorded by oscilloscope UXR0204A Keysight and used to fix the values of the RC system nodes; another signal part was fed into FB. The FB electronic part consisted of a non-inverting radio-frequency (RF) signal amplifier WYDZ-LNA-10M-6GHz 30 dB (RFA1), attenuator DYKB DC-6GHz with the attenuation coefficient varying with the 0.25 dB step (ATT), RF signal combiner SHWLCB2-204000S (COMB), inverting amplifier Mini-Circuits ZX60-V82-S + 20-6000MHz 13 dB (RFA2), signal inverter (INV), and bias treatment device Mini-Circuits ZX85-12G-S+ (BT). The input signal was fed into the system with the aid of the Keysight M8195A arbitrary-waveform generator.

The system FB strength k_{fb} is defined as the resulting gain: $k_{fb} = k_1 - k_a + k_2$, where $k_{1,2}$ is the fixed gain of RFA1 (RFA2) equal to 30 (13) dB, k_a is the variable attenuation coefficient of the attenuator used to vary the

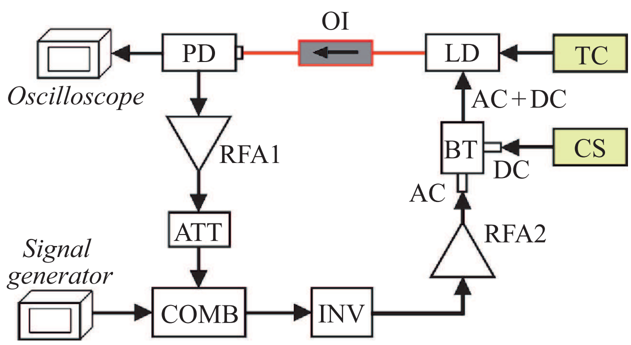

Figure 1. Schematic diagram of the optoelectronic reservoir computing system. Red lines represent the optical signal; black lines are for the electrical signal. The figure variant with colored lines is given in the paper electronic version.

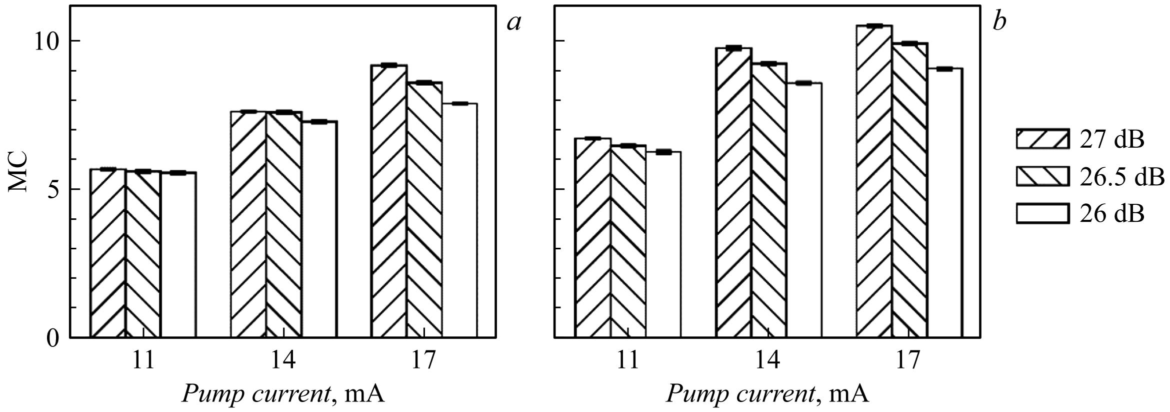

Figure 2. The system memory capacity (MC) versus the pump current and feedback strength. $N = 20$ (a) and 40 (b).

feedback strength. The FB signal delay determined experimentally by using rectangular pulses from the waveform generator is 23.8 ns, which matches the bypass frequency of 42 MHz. The RC system energy consumption is no more than 2 W (besides the energy consumption of the generator and oscilloscope).

Input signals are entered into the RC system sequentially by modulating the LD pump current. The time of entering one value $T_S = Nt_N$ is made close to the FB signal delay time but slightly different so as to eliminate resonance effects that significantly degrade the system performance [8]. To set the weights of the reservoir input layer, each input value S_i at the i-th input step is modulated during the input time by the so-called mask [5], that is, a piecewise constant function with random fixed values different at each interval t_N, which is defined for time interval T_S. The TDS system output value is created by fixing the LD radiation intensities with PD and oscilloscope at time moments related to the virtual nodes and multiplying them by the output layer weighting coefficients determined at the training phase via linear regression [5,9].

The best performance of the system under consideration was previously predicted theoretically to occur near the instability boundary of the stationary lasing mode [6,7], which was found experimentally at $k_{fb} = 27$ dB ($k_a = 16$ dB) for the pump current of 9–25 mA. The band of the laser pump current modulation by the -10 dB level is limited to the frequency of 1.4 GHz, while the FB passband is 0.01–2 GHz. The RC system characteristics were studied depending on the FB strength, LD pump current and number of the system nodes N. Symbol input frequency $1/T_S = 40$ MHz determines the pump current modulation frequency and, hence, the laser power modulation frequency as $1/t_N = 1/(T_S N) = 0.8$ and 1.6 GHz for 20 and 40 nodes, respectively. To ensure synchronous reading of virtual nodes, the PD output signals were recorded with an oscilloscope with the sampling frequency multiple to the pump current modulation frequency: 4 and 8 GHz for 20 and 40 nodes, respectively. To find standard deviation for each measured characteristic of the system, the RC process was repeated five times.

The memory capacity (MC) characterizes the systemś ability to restore the previously entered data [9]. It is defined as

$$\mathrm{MC} = \sum_{d=1}^{\infty} mc_d = \sum_{d=1}^{\infty} \frac{\mathrm{cov}^2(O_i, S_{i-d})}{\sigma^2(O_i)\sigma^2(S_i)}, \tag{1}$$

where mc_d is the memory function, cov is the covariance, O_i is the output value at the i-th input step, S_{i-d} is the input value entered d steps earlier, σ^2 is the dispersion. Memory function mc_d represents the relationship of the reservoir output data with input data entered d steps earlier [10]. The input signal was generated by a sequence of 5000 random values uniformly distributed in the [–1,1] interval. Fig. 2 presents experimental MC values versus the pump current and feedback strength. The greatest memory capacity is 10.5 for $N = 40$, $k_{fb} = 27$ dB and pump current of 17 mA. The increase in pump current leads to an increase in memory capacity, i. e. the system becomes more linear. In [3] where the physical laser-based RC system was also implemented, the memory capacity did not exceed 8. In our RC system, the memory capacity increases only slightly with the node number increase to $N = 40$, which may be due to the fact that the LD modulation bandwidth and FB passband are limited.

By solving the task of predicting a chaotic time series of the Mackey–Glass system, it is possible to evaluate the RC system ability to predict the series values one step ahead [3]. The dynamic Mackey–Glass system is defined as

$$\frac{dy(t)}{dt} = \frac{\alpha y(t-\tau)}{1 + y^{\beta}(t-\tau)} - \gamma y(t), \tag{2}$$

where $\alpha = 0.2$, $\beta = 10$, $\gamma = 0.1$ and $\tau = 17$. To obtain the time series, equation (2) was solved by the Euler method with the step of 0.17, every third point being fixed [3].

The prediction error is estimated as the normalized root mean square error (NMSE):

$$\mathrm{NMSE} = \frac{1}{L} \sum_{i=1}^{L} \frac{(Y_i - O_i)^2}{\sigma^2(Y_i)}, \tag{3}$$

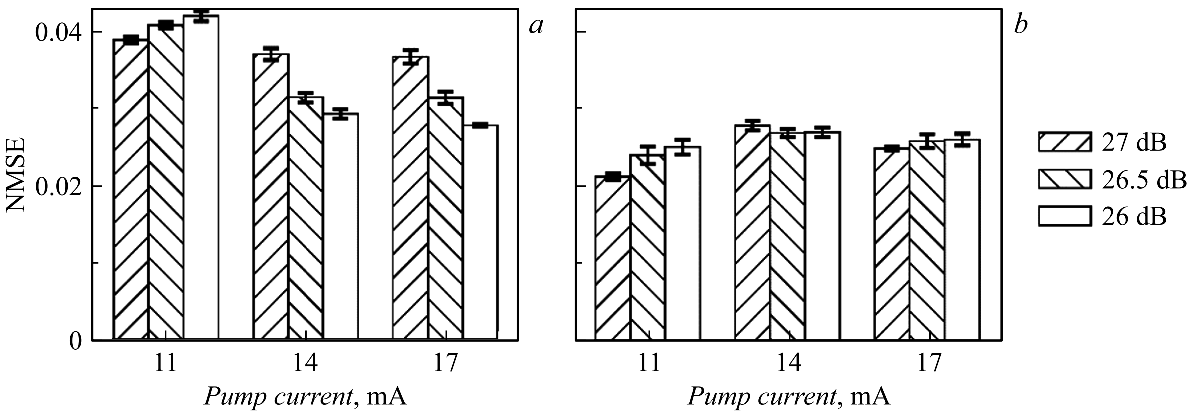

Figure 3. Error (NMSE) in predicting the time series of the Mackey−Glass chaotic system versus the pump current and feedback strength. $N = 20$ (a) and 40 (b).

where L is the test sample length equal to 1500, Y_i is the target (true) value at the time series i-th step defined by (2), O_i is the i-th step value predicted by the system. In this problem, the prediction error varies in the range of 0.02−0.04 (Fig. 3), which is comparable with the results of [1,3], while relative standard deviation does not exceed 4%, which confirms stable repeatability of calculations.

Thus, in this work we have studied experimentally a semiconductor-laser-based reservoir computing system with optoelectronic feedback, which is characterized by low power consumption (no more than 2 W). We have determined the systemś memory capacity whose maximum value is ~ 10 and solved the problem of predicting the Mackey−Glass system time series with the lowest prediction error of 0.02. The results point to perspectives of the system under consideration.

Funding

The study was supported by the Russian Science Foundation (project № 23-72-01050 (https://rscf.ru/project/23-72-01050/).

Conflict of interests

The authors declare that they have no conflict of interests.

References

[1] M.C. Soriano, P. Massuti-Ballester, J. Yelo, I. Fischer, in *ICANN 2019*: *Workshop and special sessions*, ed. by I. Tetko, V. Kůrková, P. Karpov, F. Theis. Lecture Notes in Computer Science (Springer, Cham, 2019), vol. 11731. p. 170–174. DOI: 10.1007/978-3-030-30493-5_18

[2] Y. Chen, L. Yi, J. Ke, Z. Yang, Y. Yang, L. Huang, Q. Zhuge, W. Hu, Opt. Express, **27** (20), 27431 (2019). DOI: 10.1364/OE.27.027431

[3] J. Bueno, D. Brunner, M.C. Soriano, I. Fischer, Opt. Express, **25** (3), 2401 (2017). DOI: 10.1364/OE.25.002401

[4] K. Harkhoe, G. Verschaffelt, A. Katumba, P. Bienstman, G. Van der Sande, Opt. Express, **28** (3), 3086 (2020). DOI: 10.1364/OE.382556

[5] L. Appeltant, M.C. Soriano, G. Van der Sande, J. Danckaert, S. Massar, J. Dambre, B. Schrauwen, C.R. Mirasso, I. Fischer, Nat. Commun., **2**, 468 (2011). DOI: 10.1038/ncomms1476

[6] P.S. Dmitriev, A.V. Kovalev, A. Locquet, D. Rontani, E.A. Viktorov, Opt. Lett., **45** (22), 6150 (2020). DOI: 10.1364/OL.405177

[7] G.O. Danilenko, A.V. Kovalev, E.A. Viktorov, A. Locquet, D.S. Citrin, D. Rontani, Chaos, **33** (1), 013116 (2023). DOI: 10.1063/5.0127661

[8] G.O. Danilenko, A.V. Kovalev, E.A. Viktorov, A. Locquet, D.S. Citrin, D. Rontani, Chaos, **33** (1), 113125 (2023). DOI: 10.1063/5.0172039

[9] L. Larger, A. Baylón-Fuentes, R. Martinenghi, V.S. Udaltsov, Y.K. Chembo, M. Jacquot, Phys. Rev. X, **7** (1), 011015 (2017). DOI: 10.1103/PhysRevX.7.011015

[10] H. Jaeger, *Short term memory in echo state networks*, GMD report (GMD Forschungszentrum Informationstechnik, St. Augustin, 2002), vol. 152. DOI: 10.24406/publica-fhg-291107

Translated by EgoTranslating